

MODELLING OF IMPACT DAMAGE IN LAMINATED COMPOSITES

Christophe Bouvet, Bruno Castanié, and Jean-Jacques Barrau

Université de Toulouse, Institut de Génie Mécanique,
118 route de Narbonne, 31062 Toulouse cedex 04, France
bouvet@lgmt.ups-tlse.fr

ABSTRACT

In the current paper a finite element model is developed to simulate numerically the damages (matrix cracks, delaminations and fibres failures) appearing during a low velocity / low energy impact on composite laminate panel. This model is based on experimental observations and impact damage scenario proposed by Renault [11], and in particular, the coupling between matrix cracks and delaminations which is fundamental in the damage development during impact. This model allows to account for this coupling very easily without material parameters adding.

The originality of the proposed finite elements model is to respect the material orthotropy characteristics of each ply to take into account the transverse matrix cracks or delamination cracks.

Comparisons between experimental tests performed by Aboissiere [1] and the results acquired by numerical calculations allow to validate the relevance of this model. Afterwards it is used, in interaction with experimental observations, to try to explain fundamental points of the impact damage creation like the coincidence of a delamination direction with the lower ply one, or the fibres failures effect.

1. INTRODUCTION

Composite materials have been increasingly introduced in airframe and spatial applications because of their interesting mechanical characteristics and their low specific weight. Nevertheless, for structures submitted to low energy impacts or minor objects drop (dropping tools during assembly or maintenance operation) composite laminates reveal a brittle behaviour and a drastic decrease of their residual mechanical characteristics [2-4]. Consequently, it is essential to improve the modelling of the damage developing during impact in composite laminates to better evaluate numerically their residual mechanical characteristics in order to optimise these structures design.

Although many authors tried to model the impact damage in composite laminates [5-7, 9], many works are still necessary to correctly simulate these damages and in particular delaminations between plies. Among these large studies of impact damage, many authors used internal variables of damage to simulate matrix cracks and delaminations, so these models don't allow to take into account the discontinuity phenomena like shear transverse matrix cracks or delamination cracks.

The originality of the proposed finite elements model is to respect the material orthotropy characteristics of each ply to take into account the transverse matrix cracks or delamination cracks.

2. EXPERIMENTAL BASIS OF THE MODEL

2.1 Experimental scenario of Renault on the impact damages

Among the large studies which try to explain the different damages developing in a composite laminate plate during a low velocity / low energy impact [2-4], Renault's work [9] is particularly interesting. In this work, Renault proposed a scenario of impact damages, which gives to matrix cracks a precursor role on the development of the delamination in the laminate. This scenario begins with the development of matrix cracks in the impact zone below the impactor. These cracks, of transverse direction (in (l, t) plane, where l is the longitudinal or fibre direction and t the transverse one) grew up during the loading following the fibre direction. Therefore, in each ply, a strip of

fibres and resin disjoints and slides in the normal direction of this ply (z) (fig. 1). This disjointed strip creates an interlaminar zone of tension stress between 2 consecutive plies and can induce in this zone the formation of a delamination. In fig. 1a, a schematic application of this scenario is proposed with a $[-45^\circ, 0^\circ, 45^\circ]$ stacking sequence, where -45° is the lower ply and 45° the upper ply, impacted side. This stacking sequence is not a real one but represents only a part of a real stacking. On the figure 1a, the disjoint strips of the first 2 plies are drawn and illustrate the interlaminar zone of tension stress. This zone, limited with the disjointed strips of the 2 adjacent plies, has a triangular shape with a size which grows from the impacted side to the non-impacted side. The figure 1b illustrates the interlaminar zones of tension stress between the $-45^\circ / 0^\circ$ plies and $0^\circ / 45^\circ$ plies.

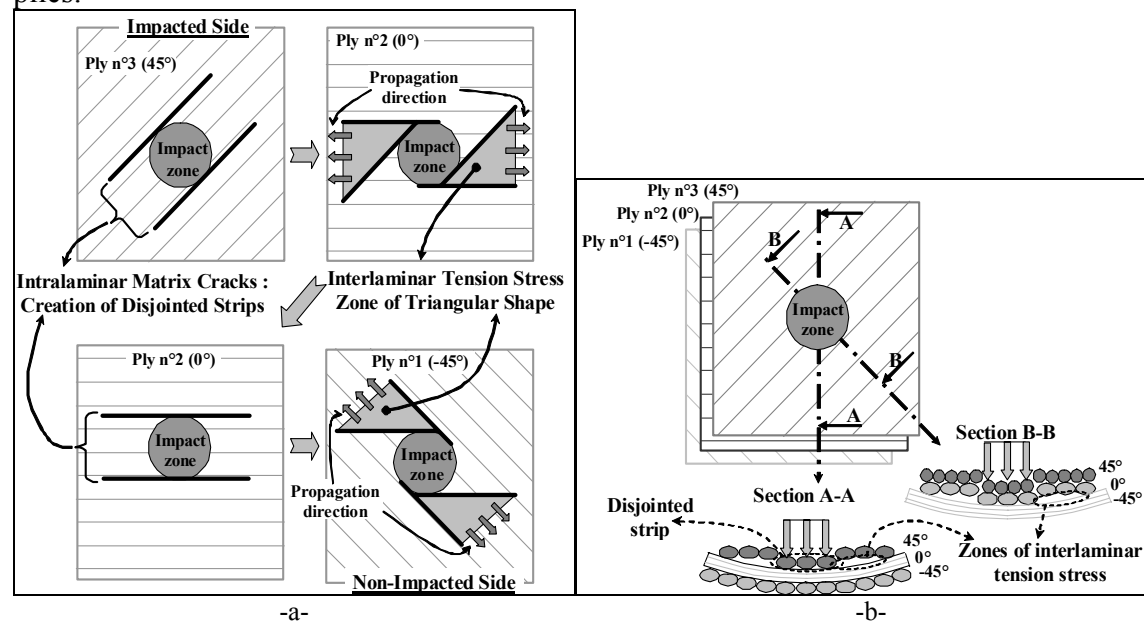


Fig. 1: Formation mechanism of delaminations (a) and interface tension stress zones (b)

Then the aim of this work is to build a model using this experimental scenario to simulate the damage which develops during the impact test.

The originality of the proposed model is to respect the material orthotropy of each ply to take into account the matrix transverse cracks, the delamination cracks and the interaction between these 2 phenomena. Then this model must allow the creation of disjointed strips due to transverse matrix cracks, the slide of these strips in order to create zones of interlaminar tension stress and the opening of these zones.

2.2 Experimental impact tests

Among the numerous experimental investigations in the literature [2-4], the Aboissiere's one [1] was used to set this model because of the following interests :

Firstly, the stacking sequence used in these tests $[0^\circ_2, 45^\circ_2, 90^\circ_2, -45^\circ_2]_S$ respects the classical stacking laws, as the mirror symmetry and no angle exceeds 45° between 2 consecutive plies. This stacking is very simple, but allows not to have a too complicated model, other model verifications are in progress on industrial sequences more realistic.

Secondly, the damage observations, in particular delaminations, were realised with ultrasonic investigation of very good quality (fig. 7) which allows to simply identify each interface. Moreover, C-Scan was equally performed on the non-impacted side (fig. 7b) which gives supplementary information on the delamination shape and in particular the exact shape of the first interface of non-impacted side.

Impact tests were performed on laminate composite $100 \times 150 \text{ mm}^2$ plates simply supported by a $75 \times 125 \text{ mm}^2$ shadow (IGC 04.26.383^{N-4} Airbus) with a spherical

impactor of 16 mm-diameter. The material used is a prepreg with carbon unidirectional fibres and epoxy matrix HTA/EH24 manufactured by HEXCEL of around 0.25 mm-thickness ply. The material characteristics evaluated by test are summarized on table 1:

| E_l (GPa) | E_t (GPa) | ν_{lt} | ε_l^f (%) | σ_t^f (MPa) | G_{lt} (GPa) | τ_{lt}^f (MPa) | G_I (N/m) |
|-------------|-------------|------------|-----------------------|--------------------|----------------|---------------------|-------------|
| 143 | 100 | 0.29 | 1.357 | 80 | 5.1 | 77 | 280±50 |

Table 1 : Material parameters

Where E_l and E_t are the Young Modulus in longitudinal and transverse direction respectively, ν_{lt} the Poisson ratio, ε_l^f the failure strain in longitudinal direction, σ_t^f the failure stress in transverse direction, G_{lt} the shear modulus, τ_{lt}^f the failure shear stress and G_I the energy release rate obtained in propagation with a $0^\circ/0^\circ$ interface.

3. NUMERICAL MODELLING

According to the Renault's scenario, the transverse matrix cracking in a ply and the delamination between 2 consecutive plies are 2 very involved phenomena. Then the model must account for these 2 phenomena and must allow their interaction which is the fundamental point in the impact damage creation.

3.1 Matrix cracking : ply model

The first damage appearing during an impact test is the matrix cracking which creates in each ply, according to the Renault's theory mentioned above, disjointed strips (fig 2). Then the ply mesh must allow the development of transverse matrix cracks and the creation of these disjointed strips. So each ply is meshed thanks to volumic elements with a side parallel to the fibres direction and one element in the thickness. And to allow the transverse matrix cracks, springs are added between 2 consecutive elements in the transverse direction (fig. 2).

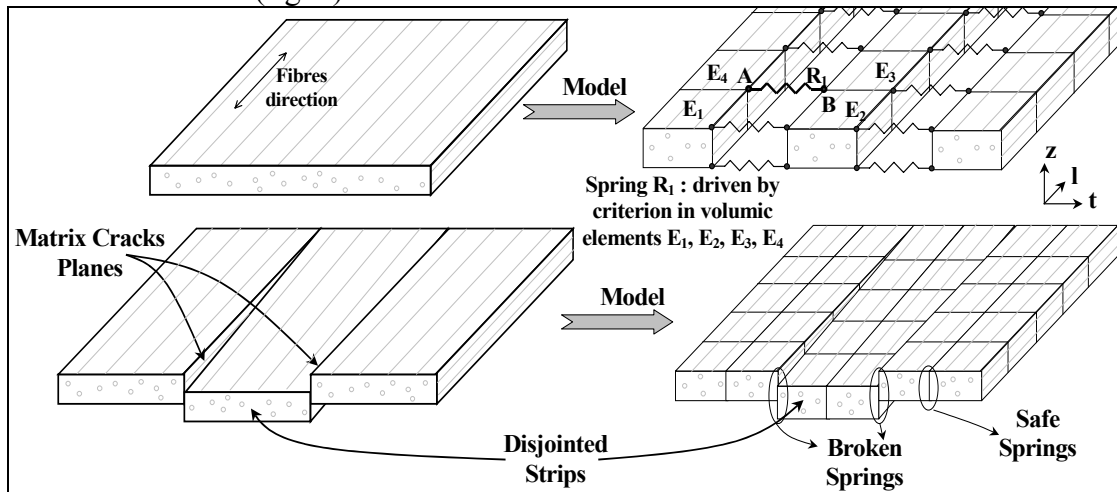


Figure 2 : Model of the ply

If there are no matrix cracks, these springs must join 2 consecutive elements in the transverse direction and if the matrix is cracked, they must let free 2 consecutive elements. Then the ply model consists in little strips meshed in the longitudinal direction, with one element in the width and one element in the depth of the ply. If no matrix cracks exit, these strips are jointed together with null length springs of very high stiffness in the 3 directions (typically 10^7 N/mm) otherwise the stiffness is put to zero. The matrix crack is driven by a classic quadratic criterion :

$$\left(\frac{\langle \sigma_t \rangle^+}{\sigma_t^f} \right)^2 + \frac{\tau_{lt}^2 + \tau_{tz}^2}{(\tau_{lt}^f)^2} \leq 1$$

where σ_t is the transverse stress, τ_{lt} and τ_{tz} the shear stresses in the (lt) and (tz) planes, $\langle \rangle^+$ the positive value and σ_t^f and τ_{lt}^f the failure stresses mentioned above. A particularity of this model is to drive this matrix cracking criterion of these springs thanks to stresses in adjacent elements and not thanks to stresses in the spring. Then criterion is evaluating in each volumic element of the ply, and a spring is broken if it is reached in at least one of its 4 neighbouring volumic elements. For example, for the spring R_1 of the figure 2, the criterion is evaluated thanks to the mean stress in the 4 volumic elements E_1, E_2, E_3, E_4 , and not to the force in the spring, which allows to avoid stress concentration in the tip of matrix cracks.

This ply model allows to correctly take into account the proposed experimental scenario in respecting the orthotropic behaviour of the ply, but it obliges to build refined and fastidious mesh. In effect this model imposes a constant size of the finite elements in the studied zone. An other particularity of this ply model is to impose a meshing of the $\pm 45^\circ$ plies with a diamond-shaped element to allow the coincidence between 2 consecutive plies (fig. 5) and only stacking sequences with $0^\circ, 90^\circ$ and $\pm 45^\circ$ plies can be meshed, which is not limiting because most industrial applications are of this type.

3.2 Delamination : Interface model

The second damage appearing during an impact test is the delaminations which detach 2 consecutive plies (fig 3). So the model must allow this behaviour and in particular if there is no interface crack, it must join 2 consecutive plies in the normal direction (z) and if the interface is cracked, it must let free 2 consecutive plies. To do this, if no interface cracks exist, 2 consecutive plies are attached together with 4 null length springs of very high stiffness (typically 10^7 N/mm in the 3 directions) otherwise the stiffness is put to zero.

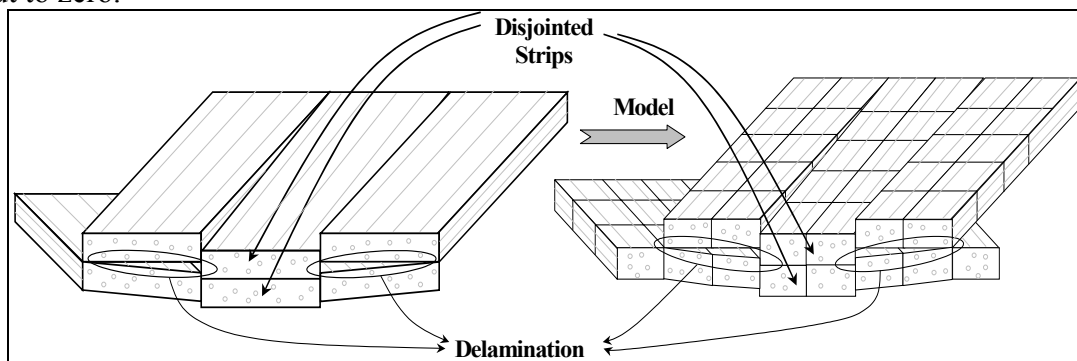


Figure 3 : Model of the interfaces

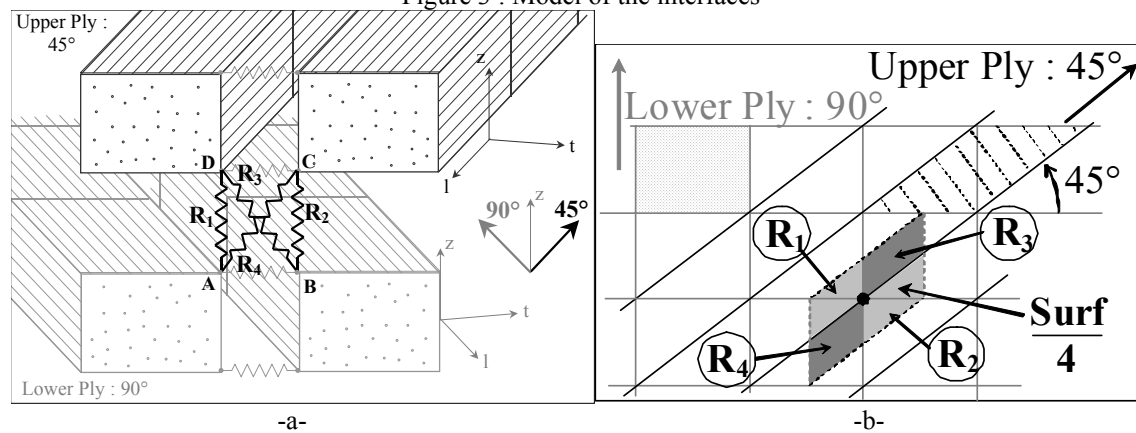


Figure 4 : The 4 springs of delamination (a) and the covered surface (b)

In effect, 4 springs are necessary (fig. 4a), because there are 2 nodes for the upper ply and 2 nodes for the lower ply. Then each spring makes the bonding between one upper ply node and one lower ply node. Physically, each spring represents one quarter of the

delamination concerned surface (fig 4b). For example on the fig. 4b, the spring R_1 between the nodes A and D represents the surface R_1 . Now a criterion must be defined to drive interface crack spring and to simulate the delamination. In order to follow the experimental scenario proposed by Renault, which explains delamination appearing by interlaminar zone of tension stress, a very simple criterion of interlaminar normal stress was used :

$$\text{For } i = 1 \text{ to } 4 : \quad (\sigma_z)_i = \frac{(F_z)_i}{\text{Surf}/4} \leq \sigma_{\text{lim}}$$

where σ_{zi} is the interlaminar normal stress in the z direction for the spring i, F_{zi} the force in the spring I, Surf the surface concerned with the group of 4 springs and σ_{lim} a limit stress of interface crack. This limit stress, fundamental for this model, is characteristic of the delamination initiation, with or without preliminary matrix cracking as well as of the delamination propagation. Then three cases of delamination can be distinguished :

- The first case is the initiation which is defined by a delamination creation without preliminary damage. In this case the limit stress σ_{lim} is chosen equal to the matrix failure stress σ_t^f (80 MPa). But practically in every simulated test this criterion is never reached before the propagation one, so only the 2 other cases are implemented.

- The second case is the propagation which is defined if a neighbouring delamination spring element is broken. Practically, each delamination spring have 4 neighbours and a delamination spring is considered in propagation if at least one of these 4 neighbours is broken. In this case, the σ_{lim} value has been identified thanks to delaminated area measured experimentally : $\sigma_{\text{lim}} = 10.5$ MPa (fig. 6b).

- The last case is a pseudo-propagation which is defined if matrix cracking preliminary exists. Practically, each delamination spring is confounded with 2 matrix cracking springs, one for the upper ply and one for the lower ply. Then a delamination spring is considered in pseudo-propagation if at least one of these 2 matrix cracking springs is broken. This condition characterizes the precursor role of matrix cracks on delamination explained by Renault and by many other authors [2, 4]. In this case, the σ_{lim} value has been chosen equal to the propagation one : $\sigma_{\text{lim}} = 10.5$ MPa.

This value of σ_{lim} could seem very low compared with the matrix failure stress ($\sigma_t^f = 80$ MPa) but represents a very different phenomenon : the failure propagation. So this limit stress should rather be compared with the energy released rate ($G_I = 280 \pm 50$ N/m) measured experimentally. Practically, a few calculation during the modelling of the impact test in paragraph 3.4, have been done in the boundary of the last interface delamination (between the 0° and 45° plies) with a VCCT method and have shown a value of energy released rate between 100 and 300 N/m. This work, which must be specified, is now in progress but seems confirming the coherence of the chosen limit stress with the energy release rate. Moreover this value is very mesh sensitive, which is very classical in failure mechanics and should be smooth with the use of softening spring. In effect, the area under the stress / displacement curves of these softening spring allows to indirectly introduce the energy release rate of the interface [10]. In the present model, this work is not taken into account and to avoid mesh size problem, all finite elements have the same size (about $2*2*0.5$ mm³) and the limit stress σ_{lim} has been identified with this mesh size.

3.3 Fibres failure

The third damage appearing during an impact test is the fibres failure which drastically decreases the material stiffness in the fibres direction. This behaviour is classically taken into account with a strain failure criterion :

$$\varepsilon_l \leq \varepsilon_l^f$$

where ε_l is the strain in the fibre direction and ε_l^f is given in table 1. When this criterion is reached, the longitudinal Young modulus E_l and the shear modulus G_{lt} , G_{tz} and G_{lz} are drastically decreased, practically divided by 20 to avoid numerical instability. This fibre criterion, which can seem secondary compared to delamination criterion, strongly influences the delamination propagation in particular in the 90° direction during the impact test mentioned below (fig. 10).

3.4 Experimental validation

Finally, this model was set up in the finite element software Samcef[®] and the Aboissiere's impact tests were simulated. The half composite plate is meshed with 1 volumic element by plies sequence of the same orientation, then 7 elements in the thickness [0°_2 , 45°_2 , 90°_2 , -45°_4 , 90°_2 , 45°_2 , 0°_2] with a double thickness element in the middle, and axial symmetry conditions around the z-axis are imposed.

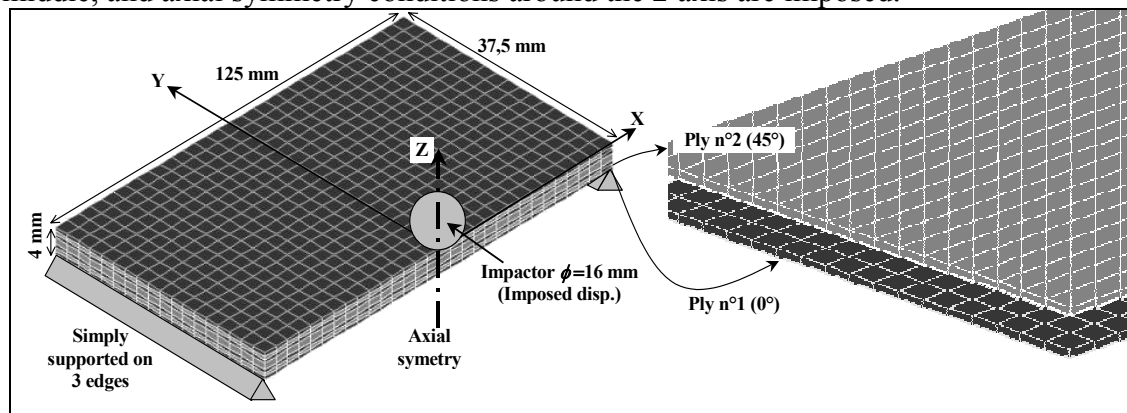


Figure 5 : Finite element mesh

The size mesh in the x direction and y direction is constant and equals about $2*2 \text{ mm}^2$. The volumic elements are after attached together by the discrete interface element mentioned above. In all, the finite element model counts 135000 degrees of freedom and the calculation lasts about 6 h on a PC dual core of 3.5 GHz with 2 Go of RAM but this size and this time should certainly be decreasing with an optimizing of the programming. Then non-linear static calculation with imposed displacement of the impactor is performed, in effect a lot of authors [8] showed the static / dynamic equivalence for this type of low velocity / low energy impacts. The displacement of the impactor, which is meshed with infinite stiffness element, is imposed between 0 and 6 mm and the displacement / force curve obtained is drawn fig. 6a. Unfortunately, this curve can't be compared to the experimental one which is not present in the Aboissiere's works. Afterwards the evolution of the delaminated surface versus impact energy, which is evaluated thanks to displacement/force curve is plotted and compared to the experimental one (fig. 6b). The correlation is very good until 5 kN and worst after, it is certainly due to the impactor perforation phenomenon which is not good simulated with the present model. In particular the perforation impactor creates fibres failures by out of plane shear (τ_{lz}) which are not taken into account by the present fibres failure criterion evaluated thanks to longitudinal strains. The simulation should overestimate the impact force and could explain a part of the difference between experiment and modelling.

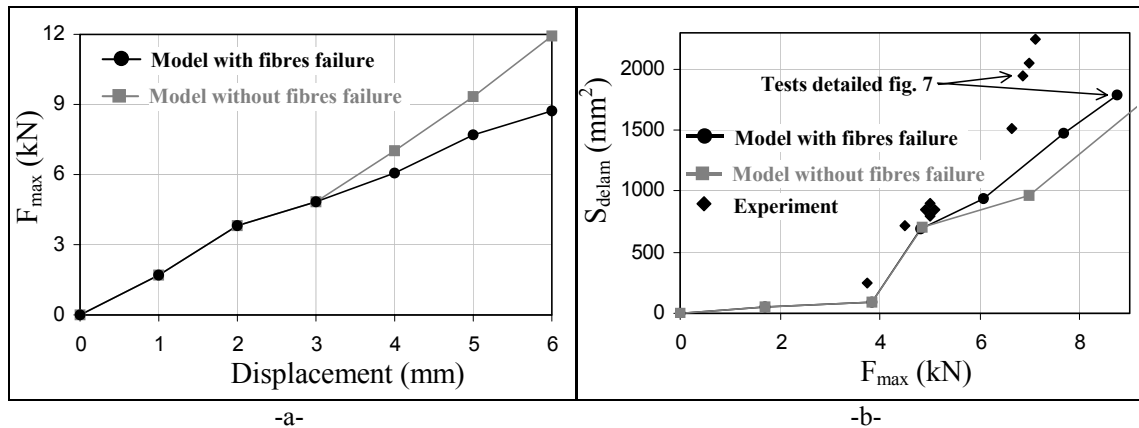


Figure 6 : Force versus displacement curve (a) and delaminated area versus impact energy curve (b) Nevertheless, the delaminated area is very insufficient to test the relevance of a modelling, the morphology of each interface gives much more information on the impact damage scenario. So the simulated delaminations are compared to the experimental one obtained by C-Scan at 25 J for experiment and 28 J for modelling (fig. 7). The greatest value for the impact energy of the model is explained by the overestimation of the impact force mentioned above. The comparison between these 2 delamination pictures are very good, the proposed modelling allows to account for a lot of experimental observations (fig. 7) :

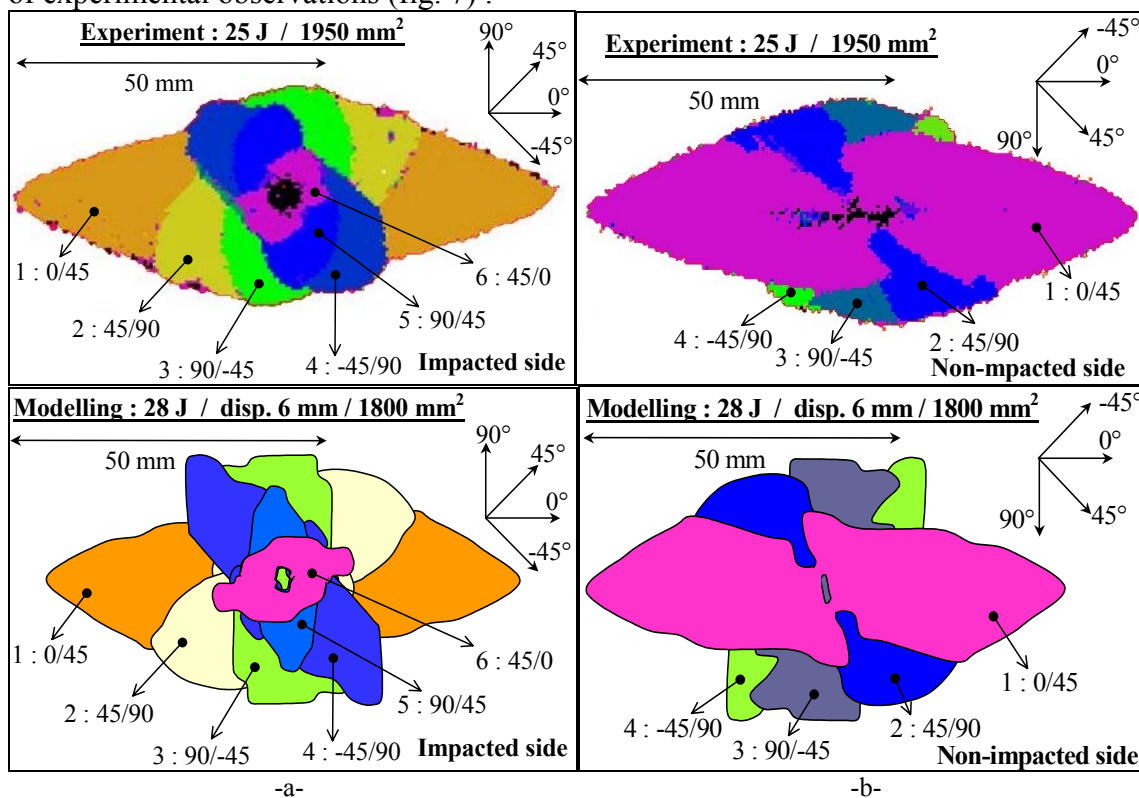


Figure 7 : Experimental and modelling delamination impacted (a) and non-impacted side (b) Firstly the propagation of a delamination is always driven by the direction of the lower ply. In effect, it is principally the tension in the fibre direction of the lower ply which creates opening of the delamination fracture. This phenomenon is very well illustrated by the figure 8. This figure represents the displacement field obtained by finite element calculation at 6 mm-displacement for two cross sections in 0° and 45° directions. It can be noted in these sections that only elements with fibres in the cross section direction are well represented. In effect, the other ones have no sides parallel to section plan which gives wrong impression of penetration between elements. Nevertheless, it can be seen on

this picture the large opening of the last delamination between the 0° and 45° obtained numerically (cross section in 0° direction). An experimental confirmation of this important opening between the last and the before last plies now in progress confirms this phenomenon.

Secondly the delaminations don't propagate (or propagate a few) in the upper ply direction of the impacted zone because there is a compression zone (fig. 8) which can be explained by the Renault's scenario. This phenomenon is well illustrated by the experimental C-Scan obtained on the non-impacted side (fig. 7b) which clearly shows the clamping of the delamination in the 45° of the impacted zone direction and it is well illustrated by the modelling.

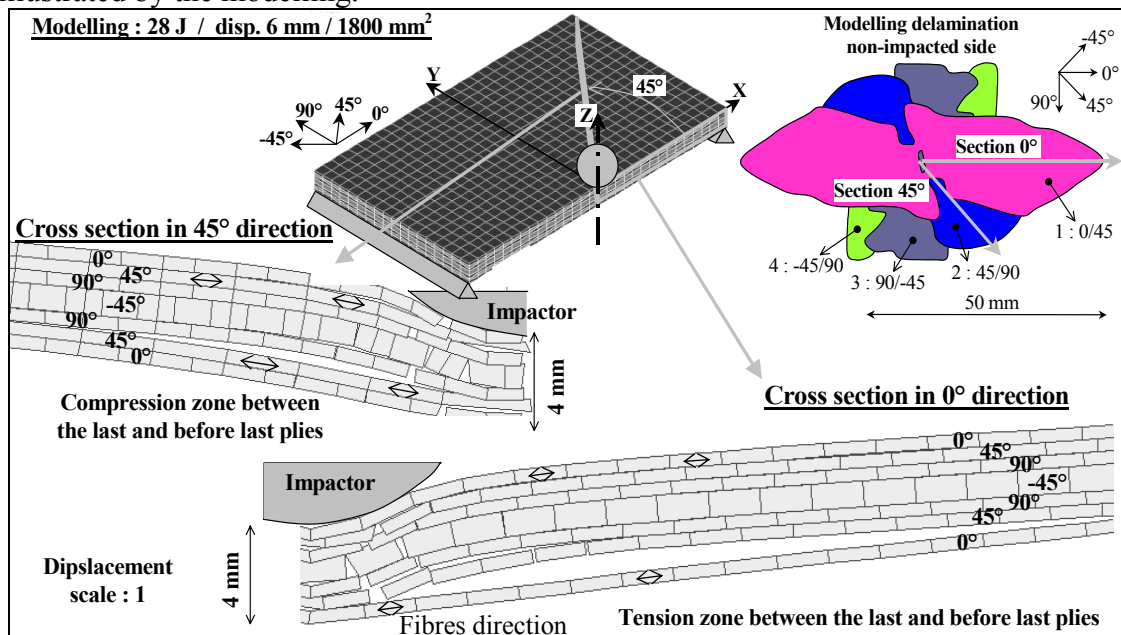


Figure 8 : Displacement response of the model

Thirdly, the global direction of the projected delaminated area is strongly directed in the 0° direction (fig. 7). This experimental observation is globally well taken into account by the model even if it gives too big delamination in the 90°. This is perhaps due to fibres failure which are imperfectly modelled by this model. It is not easy to experimentally confirm this hypothesis because the fibres failures are very difficult to observe experimentally. Nevertheless micrographic cuts or deplying [12] could allow to situate the fibres failure and to compare them with the modelling one (fig. 9), this work is now in progress.

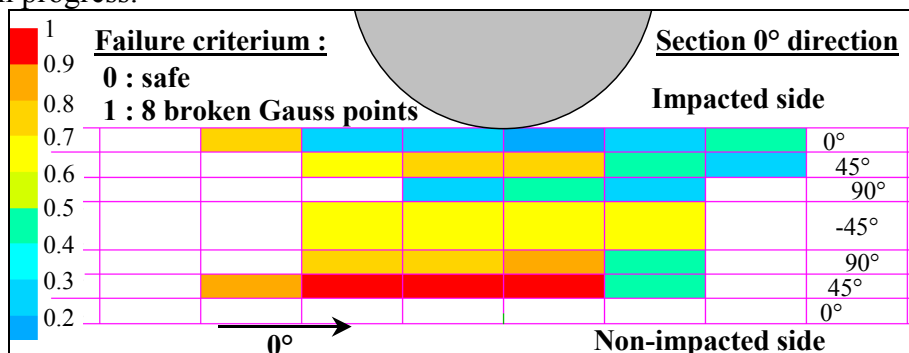


Figure 9 : Modelling fibres failures

Another possibility to indirectly confirm this hypothesis is to remove the fibre failures of the model. On the figure 10, the delamination obtained without fibre failure is drawn, and the curves force/displacement and delaminated area/impact energy are equally reported on figure 6. The lack of fibre failures increases the impact force and energy for

the same imposed displacement, and for the same displacement of 6 mm the delaminated area increases strongly from 1800 to 2850 mm². Moreover the delamination morphology is very different, the projected delaminated area is not yet directed by 0° direction but quasi-circular without the fibres failure (fig. 10). The delamination propagation in the 90° direction is so fast, it is even stopped close to the boundary conditions. This equally allows to better understand why the projected delaminated area is in the 0° direction. This is due to the rectangular shape shadow which preferentially induces fibre failures in the 45° and 90° directions, non-impacted side, because the longitudinal strains are bigger. Then, in the studied stacking sequence, the 45° and 90° plies, non-impacted side, breaks first (the 45° ply breaks before the 90° ply due to flexion effect), and decreases stresses in these directions which stops delamination propagation. And in the same time, the last 0° ply is safe, which propagates delamination in this direction.

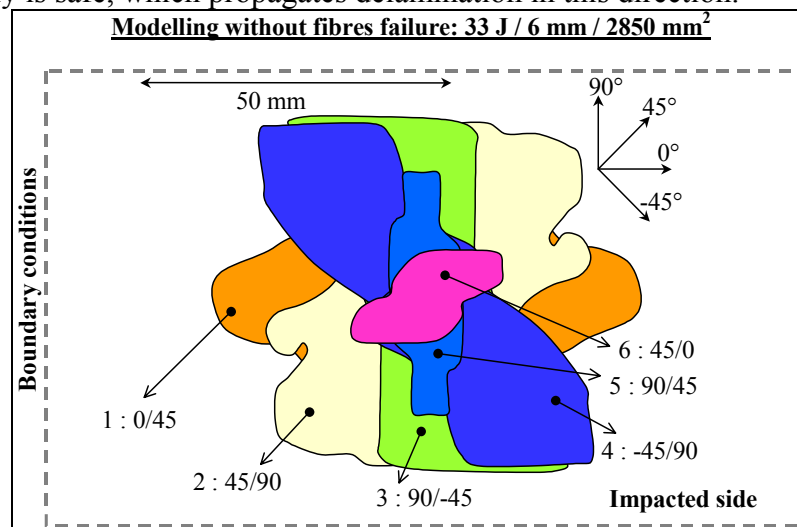


Figure 10 : Modelling delamination without fibre failure impacted side

Finally the well resemblance between the experimental and numerical damage morphology allows to conclude that the experimental considerations used to set up this model are globally representative of the physics phenomena.

4. CONCLUSION

An impact damage model has been set up to simulate the different damage types forming during an impact on composite panel. The three principal damages, which are matrix cracks, interface delamination and fibres failure, are well taken into account by the proposed model thanks to interface elements. These interface elements allow the motion between disjoint strips of fibres, the creation of tension stress at interfaces and the delamination propagation. This model, based on experimental observations and impact damage scenario proposed by Renault, should allow to better understand the physics of the delamination formation. In effect, the comparison between experimental observations and modelled phenomena and the interaction between these two, allows to explain fundamental points of the creation of the impact damage.

The first point is the importance of the fracture mode I on the delamination propagation. Indeed, the proposed model allows to take into account the delamination with only an interlaminar normal stress criterion. Even if other works must be done to study the effect of the fracture mode II on delamination propagation, the present model allows to confirm the predominance of the fracture mode I on this phenomenon.

The second one is the direction of a delamination which is always driven by the lower ply direction. Indeed this model seems to confirm this phenomenon, which is due to the creation of a disjointed strip in the interface lower ply which creates interlaminar tension stresses and delamination propagation.

The third one is the effect of fibres failure on the direction of the projected delamination. Indeed, this model seems show that fibres failures in a direction decreases stresses in this direction and induce delamination propagation in the perpendicular direction. Experimental confirmations must be done to confirm this effect, like for example the use of fibres with very different failure strain.

Nevertheless the model must be improved on the following points which are now in progress:

The use of softening springs for delamination elements to eliminate the mesh sensitivity

A new criterion for damage of fibres failure is studied

The fracture mode II will be taken into account to modelize other damage types like impact on thick plate

Afterwards this model must be improved to simulate the permanent indentation since this value is fundamental to design structures with damage tolerance.

A lot of works is still necessary to wholly simulate the damage tolerance of a composite panel and to take into account, at the same time, the damage during impact and the permanent indentation to evaluate the residual strength and to optimise the design of composite structures thanks in damage tolerance and not just with failure stress criterion.

REFERENCES

- 1 Aboissiere J., Michel L., Eve O. and Barrau J.J., "Matrix cracking and delamination under fatigue loading". *ECCM10, Brugge, Belgium, 2002*.
- 2 Abrate S., "Impact on composites structures". *Cambridge university press, 1998*.
- 3 Aoki Y., Iwahori Y., Ishikawa T., Kondo H. and Hiraoka K., 2006, "Dent depth and CAI property of CFRP laminates subjected to low velocity impact", *ECCM12, Biarritz, France, 2006*.
- 4 Davies G. A. O., Olsson R., "Impact on composite structures". *The Aeronautics Journal, v. 108, pp. 541-63, 2004*.
- 5 Finn S. R. et Springer G. S., "Delaminations in composite plates under transverse static or impact loads". *Composite Structures, Vol. 23, pp. 177-204, 1993*.
- 6 Guinard S., Allix O., Guédra-Degeorges D. and Vinet A., "A 3D damage analysis of low-velocity impacts on laminated composites". *Composite Science and Technology, Vol. 62, pp. 585-9, 2002*.
- 7 Hou J. P., Petrinic N. et Ruiz C., 2001, "A delamination criterion for laminated composites under low-velocity impact.", *Composite Science and Technology, v. 61, pp. 2069-74*.
- 8 Kwon Y. S., Sankar B. V., "indentation flexure and low velocity impact damage in graphite epoxy laminate", *Journal of Composite Technology and Research, v. 15, n. 2, pp. 101-11, 1993*.
- 9 Ladevèze P., Lubineau G. and Marsal D., "Towards a bridge between the micro- and mesomechanics of delamination for laminated composites", *Composite Science and Technology, v. 66, pp 698-712, 2006*.
- 10 Mi Y., Crisfield M. A. and Davies G. A. O.. "Progressive delamination using interface elements", *Journal of Composite Materials, v. 32, n° 14, pp. 1246-72*
- 11 Renault M. "Compression après impact d'une plaque stratifiée carbone époxyde – Etude expérimentale et modélisation éléments finis associée". *Rapport interne EADS CCR, 1994*.
- 12 Sztefek P. and Olsson R., "Tensile stiffness distribution in impacted composite laminates composite laminates determined by an inverse method", *Composites Part. A, doi: 10.1016, 2007*.